ELSEVIER

Catalysis Today 44 (1998) 333–342

CATALYSIS TODAY

Supported gold catalysis derived from the interaction of a Au–phosphine complex with as-precipitated titanium hydroxide and titanium oxide

Youzhu Yuan[a,b], Kiyotaka Asakura[c], Anguelina P. Kozlova[a], Huilin Wan[b], Khirui Tsai[b], Yasuhiro Iwasawa[a,*]

[a]*Department of Chemistry, Graduate School of Science, The University of Tokyo, Hongo, Bunkyo-ku, Tokyo 113-0033, Japan*
[b]*Department of Chemistry and State Key Laboratory of Physical Chemistry for the Solid Surface, Xiamen University, Xiamen 361005, China*
[c]*Research Center for Spectrochemistry, Graduate School of Science, The University of Tokyo, Hongo, Bunkyo-ku, Tokyo 113-0033, Japan*

Abstract

Supported gold catalysts derived from interaction of a Au–phosphine complex $Au(PPh_3)(NO_3)$ (**1**) with conventional titanium oxide TiO_2 and as-precipitated titanium hydroxide $Ti(OH)_4^*$ (*, as-precipitated) have been characterized by means of XRD, XPS, EXAFS, and ^{31}P CP/MAS–NMR. The Au complex **1** was supported on TiO_2 and $Ti(OH)_4^*$ without loss of Au–P bonding at room temperature. The Au complex **1** on TiO_2 was readily and completely decomposed to form metallic gold particles by calcination at 473 K, whereas only a small part of the complex **1** on $Ti(OH)_4^*$ was transformed to metallic gold particles. By calcination of **1**/$Ti(OH)_4^*$ at 573 K the formation of both metallic gold particles and crystalline titanium oxides became notable as evidenced by XRD, XPS and ^{31}P CP/MAS–NMR. The mean diameter of Au particles in **1**/$Ti(OH)_4^*$ calcined at 673 K was less than 30 Å as estimated from Au(2 0 0) diffraction, which was about one-tenth of that for the corresponding **1**/TiO_2. Thus the as-precipitated titanium hydroxide $Ti(OH)_4^*$ was able to stabilize the Au complex **1** to lead to the simultaneous decomposition of Au complex and $Ti(OH)_4^*$. The catalyst **1**/$Ti(OH)_4^*$ calcined at 673 K afforded remarkably high catalytic activity for low-temperature CO oxidation at 273–373 K as compared to the catalyst **1**/TiO_2.

Keywords: Supported Au phosphine complex; Supported gold catalyst; Characterization; CO oxidation

1. Introduction

It has been demonstrated that highly dispersed gold catalysts are tremendously active for low-temperature CO oxidation [1–21] and other catalytic reactions [22–31]. Au/Fe_2O_3, Au/Co_3O_4, Au/NiO, Au/Al_2O_3, and Au/SiO_2 showed an overall trend indicating that CO oxidation activity increased with decreasing size of the Au particles [5], where the size of Au particles may depend on the kind of supports due to the different Au–support interaction. Superfine Au particles may be a prerequisite for the observation of a Au–support interaction [32]. Thus to obtain highly efficient Au catalysts it is necessary to develop a new method for catalyst preparation which can control Au particle sizes and Au–support interaction during catalyst preparation.

*Corresponding author. Fax: 81 3 5800 6892; e-mail: iwasawa@chem.s.u-tokyo.ac.jp

0920-5861/98/$32.00
PII S0920-5861(98)00207-7

Use of suitable metal complexes as precursors is a promising way to prepare tailored metal catalysts with more efficient interaction between metal and support to generate unique catalysis [33–38]. To obtain highly dispersed Au particles on oxide surfaces, we chose Au–phosphine complexes $Au(PPh_3)(NO_3)$ (**1**) and $[Au_9(PPh_3)_8](NO_3)_3$ (**2**) as precursors which could be thermally decomposed on oxide surfaces [39]. When the Au complexes were supported on conventional metal oxides such as Fe_2O_3 and TiO_2, however, the supported Au complexes aggregated to large Au particles (about 300 Å in diameter) during calcination at 673 K as characterized by EXAFS, XRD, and TEM [40]. These Au complex-derived Au particles on the traditional oxides showed low catalytic activity for CO oxidation. As the Au aggregation and low activity were thought to be due to almost no or weak interaction of the Au precursors with the oxide surfaces, the oxides were exposed to water vapor to produce surface OH groups which can interact with the Au complexes. The Au complexes supported on the water-treated oxides also aggregated to large Au particles by calcination at 673 K. Next, metal hydroxides commercially available were used as the support for the Au complexes, but the obtained supported Au catalysts also showed low activities for CO oxidation.

Very recently, we [40,41] successfully developed a new way to prepare supported Au catalysts with dispersed Au particles by supporting **1** and **2** on as-precipitated wet metal hydroxides, followed by temperature-programmed calcination in a flow of air. The obtained highly dispersed Au particles on the specially obtained supports showed extremely high activity for catalytic CO oxidation at low temperatures typically at 203–273 K. On the other hand, the catalysts obtained by supporting the Au–phosphine complexes **1** and **2** on conventional metal oxides showed CO oxidation activities only at 300–500 K under the identical reaction conditions. The Cl-containing precursors such as $Au(PPh_3)Cl$ and $HAuCl_4$ were unsuitable for the preparation of highly dispersed Au particles on the supports. The characterization studies using XRD, EXAFS and TEM revealed that the as-precipitated metal hydroxides are much superior to the conventional metal oxides as supports for small Au particles. Thus it is suggested that a way to obtain highly dispersed Au particles active for the low-temperature CO oxidation is to choose a suitable Au complex as a precursor and a suitable oxide precursor with many surface OH groups which can be transformed simultaneously to Au particles and oxide support by calcination in air.

Here we report the characterization and performance of the supported gold catalysts derived from the interaction of a Au–phosphine complex **1** with conventional TiO_2 and as-precipitated $Ti(OH)_4^*$ by means of EXAFS, XRD, XPS and ^{31}P CP/MAS (cross-polarization/magic-angle spinning)–NMR.

2. Experimental

2.1. Preparation of catalyst

A Au–phosphine complex, $Au(PPh_3)(NO_3)$ (**1**), was synthesized according to the literature [42]. As-precipitated titanium hydroxide $Ti(OH)_4^*$ was prepared by hydrolysis of $Ti(i\text{-}OC_3H_7)_4$ (titanium-tetra-iso-propoxide, 99.999% purity) with an aqueous solution containing 5.0% of Na_2CO_3 (99.9% purity). The precipitate was repeatedly washed several times with deionized water until the pH reached 7.0. The as-precipitated $Ti(OH)_4^*$ was filtered, and immediately impregnated with an acetone (99.9%) solution of **1** under vigorous stirring for at least 12 h, followed by evacuation for 5 h in vacuum to remove the solvent at room temperature. The obtained samples were calcined in a glass tube at a heating rate of 4 K/min to given temperatures and the temperatures were held for 4 h under a flow of air (30 ml/min). The catalysts thus prepared are denoted as **1**/$Ti(OH)_4^*$. Note that the samples are always used as catalysts after the temperature-programmed calcination. For comparison, catalysts **1**/TiO_2 were prepared by impregnating **1** on commercially available TiO_2 (Degussa P-25), followed by temperature-programmed calcination in a similar way to that for **1**/$Ti(OH)_4^*$. The Au loading on both supports was controlled to be 3.0 wt%.

2.2. Characterization

The samples were characterized by EXAFS, XRD, XPS, and ^{31}P CP/MAS–NMR.

XRD patterns were measured on a Rigaku powder X-ray diffractometer with Cu K_α radiation over the 2θ

range 20–80°. Mean Au particle sizes for **1**/$Ti(OH)_4^*$ and **1**/TiO_2 were estimated using the Sherrer equation and the width of a selected diffraction line of Au(2 0 0). XPS spectra were recorded on a Rigaku XPS-7000 spectrometer by using MgK_α radiation with an energy of 1253.6 eV. The binding energies were referred to C(1s) at E_b=284.6 eV.

Au L_3-edge EXAFS spectra were measured in a transmission mode at BL-10B of the Photon Factory in the National Laboratory for High Energy Physics (KEK) (Proposal No.: 95G200). The measurements were carried out with a beam current of 250–350 mA and a storage-ring energy of 2.5 GeV. The samples were calcined in a U-shaped glass tube combined in a fixed-bed flow reaction system in a flow of air (30 ml/min) and transferred to EXAFS cells connected to the U-shaped glass tube. Data were analyzed by a curve-fitting method, using empirically derived phase-shift and amplitude functions. The interactions of Au–Au and Au–P were calculated by using the FEFF6.0 software [43,44]. The parameters used for the analysis are summarized in Table 1.

^{31}P CP/MAS–NMR measurements were performed at a resonance frequency of 121.616 MHz on a Chemagnetics Model-300 at room temperature. Chemical shifts were referred to $(NH_4)_2PO_4$ (1.33 ppm). Rotors were spun at 4 kHz and 4.5 μs pulses (90° pulses) were applied to obtain ^{31}P MAS spectra with proton high power decoupling. At least 1000 scans (a scan: 10 s) were acquired for each spectrum of **1**/supports. The chemical shift of triphenylphosphine in the solid state was measured as −4.9 ppm with respect to $(NH_4)_2PO_4$.

2.3. Catalytic CO oxidation

CO oxidation reactions were carried out in a fixed-bed flow reactor equipped with a computer-controlled auto-sampling system by using 200 mg of catalyst powder. The reaction gas containing 1.0% CO balanced with air purified through a molecular sieve column was passed through the catalyst bed at a flow rate of 67 ml/min (SV=20 000 ml/h/g). The reaction products were analyzed by a gas chromatograph using a column of Unibeads C for CO_2 and a column of 5A molecular sieve for CO and O_2. The material balance in the catalytic reactions was checked from the concentration of CO_2 and CO, showing good balance under all the reaction conditions tested.

3. Results

3.1. Characterization by EXAFS and XRD

EXAFS measurements in a transmission mode were carried out at room temperature to characterize **1**/TiO_2 and **1**/$Ti(OH)_4^*$. The Fourier transforms of EXAFS oscillations at Au L_3-edge for **1**/$Ti(OH)_4^*$ and **1**/TiO_2, before and after calcination at 673 K are shown in Fig. 1. The peak around 1.8 Å in spectra a and b of Fig. 1 is assignable to Au–P bond, which indicates that upon supporting the Au–phosphine complex **1** on $Ti(OH)_4^*$ and TiO_2 the Au complex **1** was not decomposed. After calcination at 673 K, the EXAFS Fourier transform peak shifted to a longer distance as shown in Fig. 1. The EXAFS curve-fitting analysis revealed that the new peak is due to Au–Au bonding. The coordination number and distance of Au–Au bond were determined to be 9.8 and 2.86 Å for **1**/$Ti(OH)_4^*$, and 11.0 and 2.87 Å for **1**/TiO_2, respectively, as shown in Table 2. No Au–P bonding was observed with the calcined samples. The results demonstrate that the Au complex on the supports was decomposed to form metallic Au particles by calcination at 673 K. The coordination numbers for **1**/$Ti(OH)_4^*$ and **1**/TiO_2 were different from each other, suggesting the formation of Au particles with different sizes.

Table 1
Crystallographic data for FEFF calculation and Fourier transform ranges used in the EXAFS analysis

FEFF calculation			Fourier transform	
Shell	N	r (Å)	Δk range ($Å^{-1}$)	Δr range (Å)
Au–P for Au(PPh_3)	1.0	2.28	3.0–14.50	1.40–2.30
Au–Au for Au foil	1.0	2.87	3.0–16.0	2.10–3.15

N: coordination number for absorber–backscatterer pair; r: distance; Δk: range for Fourier transformation (k: wave vector); Δr: range for shell isolation (r: distance).

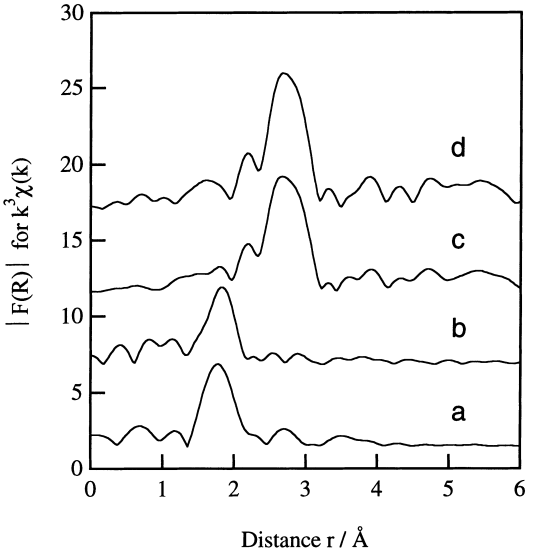

Fig. 1. The Fourier transforms of EXAFS oscillations at Au L_3-edge for **1**/TiO_2 and **1**/$Ti(OH)_4^*$ before and after calcination: (a) as-prepared **1**/$Ti(OH)_4^*$; (b) as-prepared **1**/TiO_2; (c) **1**/$Ti(OH)_4^*$ calcined at 673 K (temperature-programmed); (d) **1**/TiO_2 calcined at 673 K (temperature-programmed).

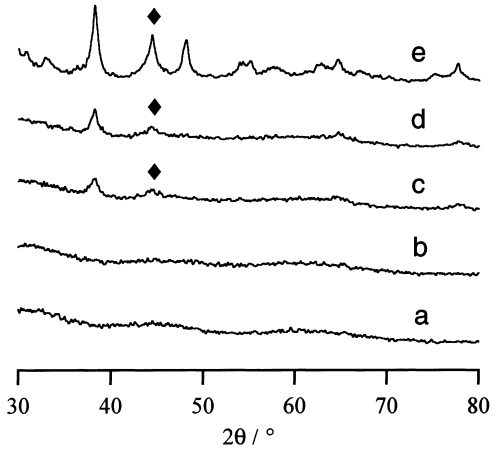

Fig. 2. The XRD patterns of **1**/$Ti(OH)_4^*$ before and after temperature-programmed calcination. (◆) Au(2 0 0): (a) as-prepared **1**/$Ti(OH)_4^*$; (b) **1**/$Ti(OH)_4^*$ after temperature-programmed calcination at 473 K; (c) **1**/$Ti(OH)_4^*$ after temperature-programmed calcination at 573 K; (d) **1**/$Ti(OH)_4^*$ after temperature-programmed calcination at 673 K; (e) **1**/$Ti(OH)_4^*$ after temperature-programmed calcination at 773 K.

The transformation from the Au–phosphine complex to metallic Au particles was accompanied by the development of the XRD peaks for crystalline TiO_2 as shown in Fig. 2. The formation of metallic gold particles and crystalline TiO_2 were not detected after calcination at 473 K, but notable after calcination at 573 K. The XRD peak for crystalline Au particles was hardly observed with **1**/$Ti(OH)_4^*$ calcined at 573 and 673 K, where the mean diameter of Au particles in **1**/$Ti(OH)_4^*$ was estimated to be less than 30 Å. In contrast, the **1**/TiO_2 catalyst showed the Au(2 0 0) peak at 2θ=44.4° after calcination even at 473 K. The mean diameter of Au particles in **1**/TiO_2 calcined at 673 K was as large as 300 Å. Moreover, the peaks for crystalline TiO_2 produced from $Ti(OH)_4^*$ were much broader than those for TiO_2 (P-25) as shown in Figs. 2 and 3.

3.2. Characterization by XPS

Fig. 4 shows the XPS spectra of P 2p and Au 4f levels in **1**/$Ti(OH)_4^*$ before and after calcination. The

Table 2
Curve-fitting results for the Au L_3-edge EXAFS data of **1**/$Ti(OH)_4^*$ and **1**/TiO_2

Pretreated temperature T (K)	Au–P				Au–Au				R_f (%)
	N	r (Å)	$\Delta\sigma^2$ (Å^2)	ΔE (eV)	N	r (Å)	$\Delta\sigma^2$ (Å^2)	ΔE (eV)	
1/$Ti(OH)_4^*$									
293	1.4±0.3	2.20±0.01	0.0006	−3.46	—	—	—	—	1.3
673	—	—	—	—	9.8±1.0	2.86±0.01	0.0001	2.55	0.9
1/TiO_2									
293	1.3±0.3	2.22±0.01	0.0000	−4.05	—	—	—	—	0.9
673	—	—	—	—	11.0±1.0	2.87±0.01	0.0001	2.12	0.7

EXAFS data of complex **1**. Au–P: N=1, r=2.20 Å.

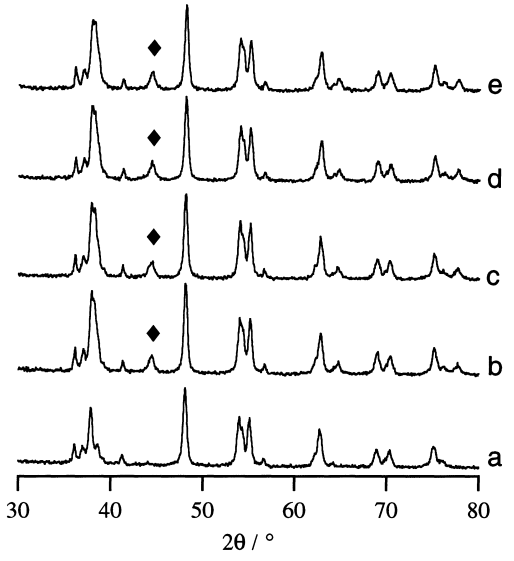

Fig. 3. The XRD patterns of **1**/TiO_2 before and after calcination. (◆) Au(2 0 0): (a) as-prepared **1**/TiO_2; (b) **1**/TiO_2 after temperature-programmed calcination at 473 K; (c) **1**/TiO_2 after temperature-programmed calcination at 573 K; (d) **1**/TiO_2 after temperature-programmed calcination at 673 K; (e) **1**/TiO_2 after temperature-programmed calcination at 773 K.

Au 4f peak in the intact **1**/$Ti(OH)_4^*$ was observed at 85.5 eV, indicating that the Au atoms were still situated as monocationic ions probably bound to the phosphine ligand. After calcination at 473 K, the Au 4f peak intensity became weak and a new peak at 83.8 eV appeared. This may be due to the coexistence of metallic gold particles and undecomposed Au complex in the sample. When **1**/$Ti(OH)_4^*$ was calcined at 573 K, no peak at 85.4 eV was observed and a peak at 83.8 eV due to metallic gold developed. The increase in the peak intensity at 83.8 eV for metallic gold species by increasing calcination temperature from 573 to 673 K may be due to the growth and dispersion of the small metallic particles on the catalyst surfaces. For the P 2p XPS spectra for phosphine species in the intact **1**/$Ti(OH)_4^*$, a peak at 131.9 eV was observed, which is assignable to the PPh_3 moiety bonding to Au. This species was also observed after calcination at 473 K. The results indicate that little change occurred significantly in the phosphine species. The peak at 131.9 eV shifted to higher binding energies (133.6–133.8 eV) by calcining the samples at 573–673 K, indicating the oxidation of phosphine species by calcination.

Fig. 5 depicts the XPS spectra of P 2p and Au 4f for **1**/TiO_2 before and after calcination. The Au 4f peak at 84.8 eV for the intact **1**/TiO_2 shifted to a lower binding energy of 83.7 eV by calcination at 473 K. No peak for the Au complex was observed with the sample calcined at 473 K. The P 2p XPS spectra showed that the

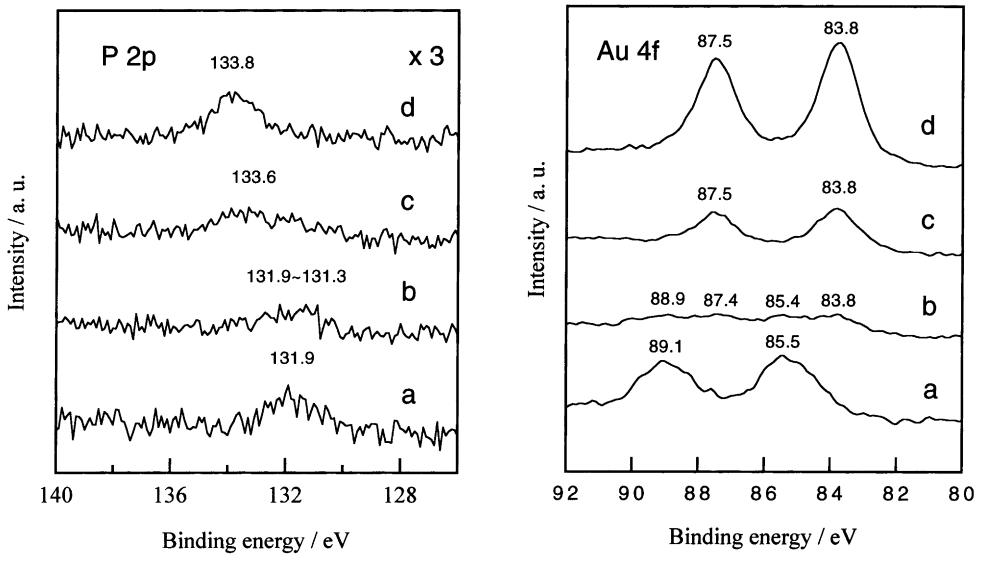

Fig. 4. P 2p and Au 4f XPS spectra for **1**/$Ti(OH)_4^*$: (a) as-prepared sample; (b) after temperature-programmed calcination at 473 K; (c) after temperature-programmed calcination at 573 K; (d) after temperature-programmed calcination at 673 K.

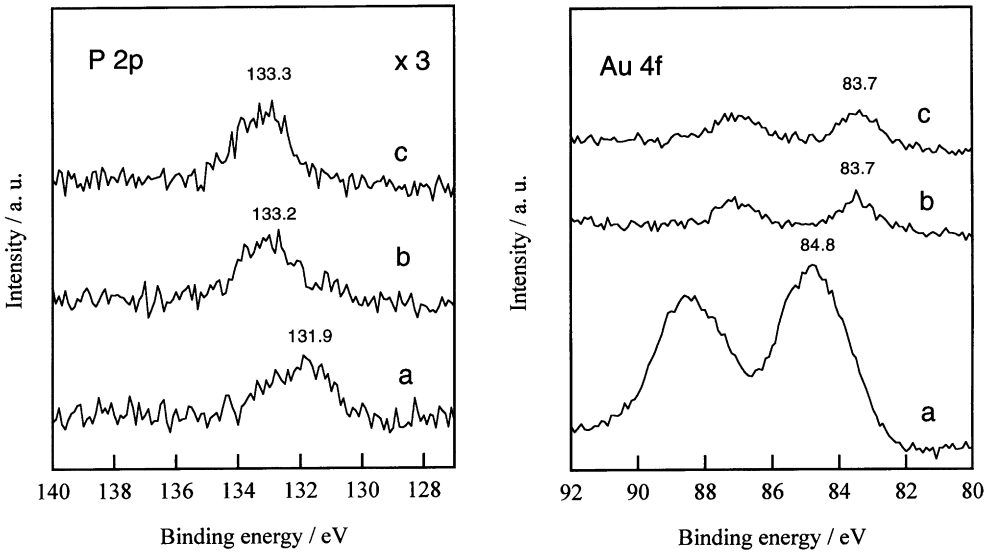

Fig. 5. P 2p and Au 4f XPS spectra for **1**/TiO_2: (a) as-prepared sample; (b) after temperature-programmed calcination at 473 K; (c) after temperature-programmed calcination at 573 K.

peak at 131.9 eV in the intact **1**/TiO_2 shifted to a higher binding energy of 133.2 eV by calcination at 473 K, suggesting that the oxidation of phosphine species occurred in parallel to the formation of metallic gold particles.

3.3. Characterization by ^{31}P CP/MAS–NMR

The effects of calcination temperatures on the ^{31}P CP/MAS–NMR spectra for **1**/$Ti(OH)_4^*$ and **1**/TiO_2 are shown in Figs. 6 and 7, respectively. The spectra for both **1**/$Ti(OH)_4^*$ and **1**/TiO_2 calcined at 473 K are similar to that for complex **1**, though the chemical shift slightly moved from 24.7 ppm (complex) to 30.6–31.6 ppm (**1**/$Ti(OH)_4^*$). The change in the chemical shift may be due to the chemical interaction between Au complex and $Ti(OH)_4^*$. No other resonances such as adsorbed PPh_3 ($PPh_3/Ti(OH)_4^*$, δ −18.8 ppm) and free PPh_3 (δ −4.9 ppm) liberated from the complex **1** were observed. After calcination at 673 K, a new resonance at 5.9 ppm was observed as shown in Fig. 6. For **1**/TiO_2, the chemical shift of ^{31}P in the intact sample was similar to that of **1**/$Ti(OH)_4^*$ (Fig. 7(a)), but new resonances with chemical shifts at 75.1, 42.5 and 10.0 ppm appeared in the NMR spectrum of **1**/TiO_2 calcined at 473 K (Fig. 7(b)). By calcination at 673 K, another new signal at 3.0 ppm

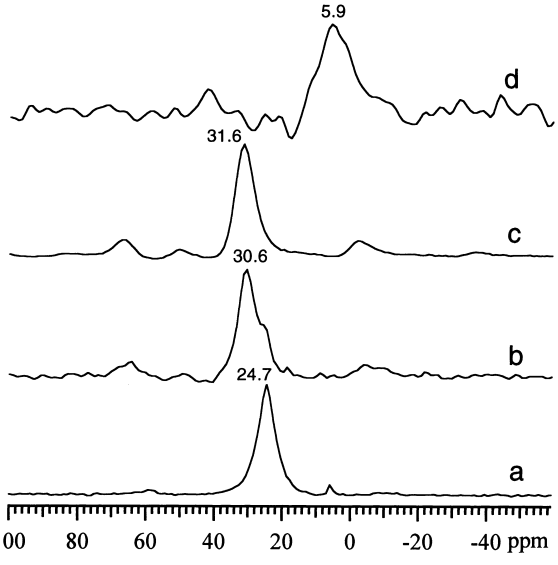

Fig. 6. ^{31}P CP/MAS–NMR spectra of **1**/$Ti(OH)_4^*$: (a) Au phosphine complex **1**; (b) as-prepared **1**/$Ti(OH)_4^*$; (c) after temperature-programmed calcination at 473 K; (d) after temperature-programmed calcination at 673 K.

was observed. We assign the peaks at 3–6 ppm (Fig. 6(d) and Fig. 7(c)) to surface $(PO_4)^{3-}$ from comparison with the spectrum of H_3PO_4/TiO_2 (Fig. 7(d)). The difference in the chemical shifts

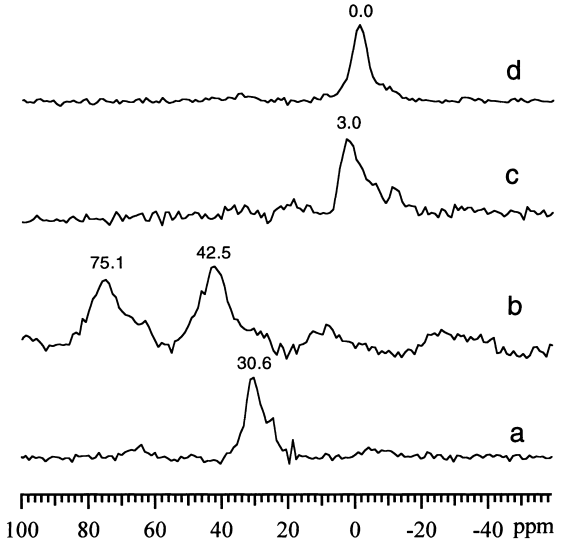

Fig. 7. ^{31}P CP/MAS–NMR spectra of **1**/TiO_2: (a) as-prepared **1**/TiO_2; (b) after temperature-programmed calcination at 473 K; (c) after temperature-programmed calcination at 673 K; (d) as-prepared H_3PO_4/TiO_2.

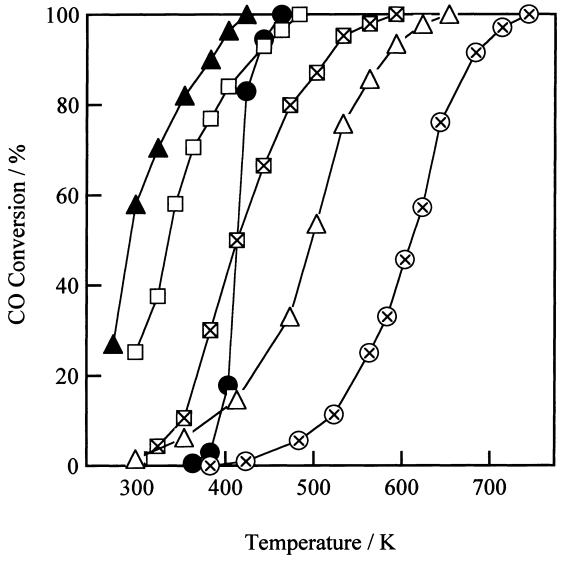

Fig. 8. CO oxidation reactions on various Au/Ti-oxide catalysts in a fixed-bed reactor (SV=20 000 ml/h/g) as a function of reaction temperature: (▲) **1**/$Ti(OH)_4^*$ (temperature-programmed calcination at 673 K); (□) **1**/$Ti(OH)_4^*$ (temperature-programmed calcination at 773 K); (●) **1**/$Ti(OH)_4^*$ (temperature-programmed calcination at 473 K); (⊠) **1**/TiO_2 (temperature-programmed calcination at 773 K); (△) **1**/TiO_2 (temperature-programmed calcination at 673 K); (⊗) **1**/TiO_2 (temperature-programmed calcination at 473 K).

may be due to the difference in the concentrations of moisture in the samples [45].

3.4. Catalytic activities

Fig. 8 depicts the catalytic activities (CO conversion) of supported Au catalysts, **1**/$Ti(OH)_4^*$ and **1**/TiO_2, for CO oxidation in a fixed-bed flow reactor as a function of reaction temperature. Under the present reaction conditions (SV=20 000 ml/h/g-cat; CO=1%), 100% conversion corresponds to a reaction rate of 8.93×10^{-3} mol/h/g-cat. It was found that the catalytic performances of **1**/$Ti(OH)_4^*$ and **1**/TiO_2 were remarkably affected by catalyst calcination temperatures. The CO oxidation on **1**/$Ti(OH)_4^*$ calcined at 673 and 773 K occurred at temperatures lower than 273 K. On the other hand, the catalysts **1**/TiO_2 calcined at 673 and 773 K were active for the CO oxidation only above 350 K. It was found that the catalytic activity of **1**/$Ti(OH)_4^*$ was much higher than that of **1**/TiO_2. When the catalyst **1**/$Ti(OH)_4^*$ calcined at 473 K was used, the CO conversion increased steeply with reaction temperature above 400 K. This might be due to an increase in the amount of small gold particles in the catalyst during the catalytic reaction by decomposition of the remaining Au complex in **1**/$Ti(OH)_4^*$ calcined at 473 K. It coincides with the observations of EXAFS, XRD and XPS for **1**/$Ti(OH)_4^*$ calcined at 473 K.

4. Discussion

The curve-fit results of the EXAFS data in Table 2 reveal that the Au–P bond lengths for **1**/$Ti(OH)_4^*$ and **1**/TiO_2 before calcination range between 2.20 and 2.22 Å. The Au–P distances are similar to that for crystalline $Au(PPh_3)(NO_3)$ [46]. The results of XRD (Fig. 2(a) and Fig. 3(a)), XPS (Fig. 4(a) and Fig. 5(a)) and ^{31}P CP/MAS–NMR (Fig. 6(a) and Fig. 7(a)) demonstrate that the Au phosphine complex $Au(PPh_3)(NO_3)$ (**1**) is supported on the surfaces of as-precipitated titanium hydroxides and titanium oxides without significant loss of the Au–P bond at room temperature. The complex–surface interaction might occur through the nitrate anions which reacted with

the surface OH groups to form surface Au–phosphine complexes $[Au(PPh_3)]^+$ as suggested from the comparison of the IR spectrum of Au phosphine complex **1** in KBr with that of the supported complex.[1] Thus, the downfield chemical shift observed in the ^{31}P CP/MAS–NMR spectra (Fig. 6(a) and Fig. 7(a)) of **1**/$Ti(OH)_4^*$ and **1**/TiO_2 may be due to the interaction between $[Au(PPh_3)]^+$ and the supports. When **1**/$Ti(OH)_4^*$ was calcined at 473 K, only a partial cleavage of the Au–P bond occurred to form a small amount of metallic gold species, but no oxidation of the phosphine species was observed, judging from the results of XRD (Fig. 2(b)), XPS (Fig. 4(b)) and ^{31}P CP/MAS–NMR (Fig. 6(b)). The results indicate that the amorphous as-precipitated $Ti(OH)_4^*$ interacts with the Au phosphine complex to stabilize the supported complex. It was found that the formation of metallic gold particles and the transformation of the amorphous $Ti(OH)_4^*$ support to crystalline titanium oxide took place at 573 K in the case of **1**/$Ti(OH)_4^*$ as evidenced by XRD (Fig. 2(c)) and XPS (Fig. 4(c)). On the other hand, when **1**/TiO_2 was calcined at 473 K, the interpretation of the newborn chemical shifts at 75.1, 42.5 and 10.0 ppm in ^{31}P CP/MAS–NMR (Fig. 7(b)) is not clearly done at present. The Au clusters such as $[Au_9(PPh_3)_8]^{3+}$ and $[Au_8(PPh_3)_7]^+$ provide similar ^{31}P-NMR shifts in the solid state [47–49]. Hence, a possible explanation for the chemical shifts at 75.1 and 42.5 is that phosphine species were bound to Au clusters/particles formed by the decomposition of the Au complex **1** at 473 K. Another possible explanation is that partial oxidation of the phosphine species on the support occurred as suggested by XPS (Fig. 5(b)).

It may be of interest to note that the intensity of the Au 4f and P 2p XPS signals for **1**/$Ti(OH)_4^*$ significantly decreased after temperature-programmed calcination at 473 K as shown in Fig. 4(b). The reason for the intensity reduction by the 473 K calcination is not clear at present, but it may not be artificial because the intensity of the O1s XPS signal (not shown) was similar in all the samples treated in Fig. 4. We propose that the reduction in the Au and P XPS signals is due to the change of the location of the Au phosphine species from the catalyst surface to the subsurface/the bulk near the surface upon calcination at 473 K. The occlude Au species are decomposed to metallic Au particles after calcination at 573 K as shown in Fig. 4(c), and the intensity increased, indicating that a part of them is moved to and dispersed at the surface. After calcination at 673 K, Au particles are suggested to be grown and dispersed at the support surface judging from the increase in the XPS signals (Fig. 4(d)).

Our previous studies [39–41,50,51] demonstrated that the Au complex on the oxide supports decomposes to metallic Au particles at lower temperatures than 573 K. In the similar temperature range the as-precipitated wet metal hydroxides are dehydrated to form anhydrous metal hydroxides, and mostly to partially dehydrated metal oxides. The supported Au complex is expected to be stabilized on the surface of the as-precipitated metal hydroxides like $Ti(OH)_4^*$ by chemical interaction between $[Au(PPh_3)]^+$ and hydroxyl groups or adsorbed water. During the calcination of the samples the decompositions of both the Au complex and the as-precipitated $Ti(OH)_4^*$ occur in parallel, which leads to the formation of highly dispersed Au particles on the in situ prepared oxide surfaces. On the other hand, in the case of **1**/TiO_2, there is only a limited number of OH groups on the oxide surface and the property of the OH groups seems to be different from the OH groups of $Ti(OH)_4^*$, and the interaction of the TiO_2 surface with the Au complex may be insufficient and weak, hence leading to aggregation to large Au particles without significant stabilization of Au species during the calcination.

When the as-prepared **1**/$Ti(OH)_4^*$ was calcined at a temperature-programmed rate of 4 K/min up to 673 K in a flow of air, it was found that the obtained Au catalysts showed high catalytic activities for CO oxidation at low temperatures like 273 K as shown in Fig. 8. The diameter of the Au particles in **1**/$Ti(OH)_4^*$ is likely to be 30 Å, judging from negligible Au(2 0 0) peak. EXAFS (Fig. 1 and Table 2) and XRD (Figs. 2 and 3) estimate the size of Au particles in **1**/$Ti(OH)_4^*$ to be about one-tenth of that in **1**/TiO_2.

Calcination of **1**/$Ti(OH)_4^*$ at 673 K oxidized the phosphine ligands to phosphoric species as suggested by XPS (Fig. 4) and ^{31}P CP/MAS–NMR (Fig. 6). There was no correlation between the catalytic activity and the amount of the phosphoric species in the catalysts, but limited information in the present study

[1]The data are obtainable upon request.

indicates the negative effect of the remaining phosphoric species on the CO oxidation catalysis.

Hoflund and co-workers [13,52] claimed that nonmetallic Au species is responsible for the low-temperature activity. Haruta et al. [6] reported that the sample having both metallic and nonmetallic Au species was not more active than the sample having only metallic Au species. Recently, it was suggested by XPS and ISS that the near-surface region of Au/Fe_2O_3 contains more Au as compared with that of Au/Co_3O_4, where Au is present as crystallites and small amounts of nonmetallic Au species are also present [52]. The present XPS date provided no evidence on the presence of cationic Au species on the surface of **1**/$Ti(OH)_4^*$, although XPS cannot detect a small amount of cationic Au species which coexists with metallic species in the 3.0 wt% Au catalysts.

5. Conclusions

The Au–phosphine complex **1** was supported intact on the surfaces of as-precipitated $Ti(OH)_4^*$ and TiO_2 at room temperature. The amorphous as-precipitated wet $Ti(OH)_4^*$ which contains large amounts of surface OH groups and physisorbed water, interacts with the Au complex **1** more efficiently than the conventional TiO_2. The transformation of the as-prepared **1**/$Ti(OH)_4^*$ to crystalline titanium oxide was observed at 573 K, whereas the decomposition of **1**/TiO_2 accompanying the oxidation of phosphine species occurred by calcination at 473 K. The difference of the decomposition behavior results in the difference of the sizes of metallic Au particles formed on **1**/$Ti(OH)_4^*$ and **1**/TiO_2 by calcination at 673 K. The mean diameter of Au particles in **1**/$Ti(OH)_4^*$ was ten times smaller than that in **1**/TiO_2. The supported Au catalysts prepared from **1**/TiO_2 catalyzed CO oxidation above 350 K, while the catalysts derived from **1**/as-precipitated $Ti(OH)_4^*$ showed a high activity for CO oxidation at low temperatures.

References

[1] M.J. Fuller, M.E. Warwich, J. Catal. 34 (1974) 445.
[2] G.C. Bond, L.R. Molloy, M.J. Fuller, J. Chem. Soc., Chem. Commun. (1975) 796.
[3] G. Croft, M.J. Fuller, Nature 269 (1977) 585.
[4] M. Haruta, T. Kobayashi, H. Sano, N. Yamada, Chem. Lett. (1987) 405.
[5] M. Haruta, N. Yamada, T. Kobayashi, S. Iijima, J. Catal. 115 (1989) 301.
[6] M. Haruta, S. Tsubota, T. Kobayashi, H. Kageyama, M.J. Genet, B. Delmon, J. Catal. 144 (1993) 175.
[7] S. Tsubota, A. Ueda, H. Sakurai, T. Kobayashi, M. Haruta, ACS Symp. Ser. 552 (1994) 420.
[8] T. Boccuzi, S. Tsubota, M. Haruta, J. Elec. Spectrosc. Relat. Phenom. 64/65 (1993) 241.
[9] M. Haruta, S. Tsubota, T. Kobayashi, A. Ueda, H. Sakurai, M. Ando, Stud. Surf. Sci. Catal. 75 (1993) 2657.
[10] S.D. Gardner, G.B. Hoflund, M.R. Davidson, D.R. Schryer, J. Catal. 115 (1989) 132.
[11] S.D. Gardner, G.B. Hoflund, D.R. Schryer, B.T. Upchurch, J. Phys. Chem. 95 (1991) 835.
[12] D.R. Schryer, B.T. Upchurch, B.D. Sidney, K.G. Brown, G.B. Hoflund, K.R. Herz, J. Catal. 130 (1991) 314.
[13] S.D. Gardner, G.B. Hoflund, D.R. Schryer, J. Schryer, B.T. Upchurch, E.J. Kielin, Langmuir 7 (1991) 2135.
[14] S.D. Gardner, G.B. Hoflund, M.R. Davidson, H.A. Laitinen, D.R. Schryer, B.T. Upchurch, Langmuir 7 (1991) 2140.
[15] G.B. Hoflund, S.D. Gardner, D.R. Schryer, B.T. Upchurch, E.J. Kielin, Appl. Catal. B 6 (1995) 117.
[16] S. Imamura, H. Sawada, K. Uemura, S. Ishida, J. Catal. 109 (1988) 198.
[17] S. Imamura, S. Yoshie, Y. Ono, J. Catal. 115 (1989) 258.
[18] S.D. Lin, M. Bollinger, M.A. Vannice, Catal. Lett. 17 (1993) 245.
[19] A. Knell, P. Barnickel, A. Baiker, A. Wokaun, J. Catal. 137 (1992) 306.
[20] A. Baiker, M. Maciejewski, S. Tagliaferri, P. Hug, J. Catal. 151 (1995) 407.
[21] G. Srinivas, J. Wright, C.-S. Bai, R. Cook, Stud. Surf. Sci. Catal. 101 (1996) 427.
[22] M. Haruta, A. Ueda, A. Tsubota, R.M. Torres Sanchez, Catal. Today 29 (1996) 443.
[23] S. Naito, M. Tanimoto, J. Chem. Soc., Chem. Commun. (1988) 832.
[24] D. Andreeva, V. Idakiev, T. Tabakova, A. Andreev, J. Catal. 158 (1996) 354.
[25] D. Andreeva, V. Idakiev, T. Tabakova, A. Andreev, R. Giovanoli, Appl. Catal. A 134 (1996) 275.
[26] H. Sakurai, A. Ueda, T. Kobayashi, M. Haruta, J. Chem. Soc., Chem. Commun. (1997) 271.
[27] H. Sakurai, S. Tsubota, M. Haruta, Appl. Catal. A 102 (1993) 125.
[28] H. Sakurai, M. Harura, Catal. Today 29 (1996) 361.
[29] H. Sakurai, M. Haruta, Appl. Catal. A 127 (1995) 93.
[30] M. Shibata, N. Kawata, T. Masumoto, H. Kimura, J. Chem. Soc., Chem. Commun. (1988) 154.
[31] S. Qiu, R. Onishi, M. Ichikawa, J. Phys. Chem. 98 (1994) 2719; Y. Takita, T. Imamura, Y. Mizuhara, Y. Abe, T. Ishihara, Appl. Catal. B 1 (1992) 79.
[32] G.C. Bond, P.A. Sermon, Gold Bull. 6 (1973) 102.
[33] Y.I. Yermakov, B.N. Kuznetsov, V.A. Zakharov, Catalysis by Supported Complexes, Elsevier, Amsterdam, 1981.

[34] J.M. Basset, J. Mol. Catal. 21 (1983) 95.
[35] Y. Iwasawa (Ed.), Tailored Metal Catalysts, Reidel, Netherlands, 1986.
[36] G. Maire, Stud. Surf. Catal. 29 (1986) 509.
[37] B.C. Gates, Chem. Rev. 95 (1995) 511.
[38] Y. Iwasawa, Proceedings of the 11th International Congress on Catalysis, Baltimore, 1996, Studies on Surface Science and Catalysis, vol. 101, p. 21.
[39] Y. Yuan, K. Asakura, H. Wan, K. Tsai, Y. Iwasawa, Catal. Lett. 42 (1996) 15.
[40] Y. Yuan, A.P. Kozlova, K. Asakura, H. Wan, K. Tsai, Y. Iwasawa, J. Catal. 170 (1997) 191.
[41] Y. Yuan, K. Asakura, H. Wan, K. Tsai, Y. Iwasawa, Chem. Lett. 9 (1996) 756.
[42] A.M. Mueting, B.D. Alexander, P.D. Boyle, A.L. Casalnuovo, L.N. Ito, B.J. Johnson, L.H. Pignolet, in: R.N. Grimes (Ed.), Inorganic Synthesis, vol. 29, Wiley, New York, 1992, p. 280.
[43] J.J. Rehr, L.J. de Mustre, S.I. Zabinsky, R.C. Albers, J. Am. Chem. Soc. 113 (1991) 5235.
[44] Y. Iwasawa (Ed.), X-Ray Absorption Fine Structure for Catalysts and Surfaces, World Scientific, Singapore, 1996.
[45] J.H. Lunsford, P.R. William, S. Wenxia, J. Am. Chem. Soc. 107 (1985) 1540.
[46] P.F. Barron, L.M. Engelhardt, P.C. Healy, J. Oddy, A.H. White, Aust. J. Chem. 40 (1987) 1545.
[47] J.W. Diesveld, E.M. Menger, H.T. Edzes, W.S. Veeman, J. Am. Chem. Soc. 102 (1980) 7935.
[48] J.W.A. van der Velden, P.T. Beurskens, J.J. Bour, W.P. Bosman, J.H. Noordik, M. Kolenbrander, J.A.K.A. Buskes, Inorg. Chem. 23 (1984) 146.
[49] N.J. Clayden, C.M. Dobson, K.P. Hall, D. Michael, P. Mingos, D.J. Smith, J. Chem. Soc., Dalton Trans. (1985) 1811.
[50] Y. Yuan, K. Asakura, H. Wan, K. Tsai, Y. Iwasawa, Chem. Lett. 2 (1996) 129.
[51] Y. Yuan, K. Asakura, H. Wan, K. Tsai, Y. Iwasawa, J. Mol. Catal. A 122 (1997) 147.
[52] W.S. Epling, G.B. Hoflund, J.F. Weaver, S. Tsubota, M. Haruta, J. Phys. Chem. 100 (1996) 9929.